Cellular Signalling 54 (2019) 122–129

Contents lists available at ScienceDirect

Cellular Signalling

journal homepage: www.elsevier.com/locate/cellsig

Upregulated BMP-Smad signaling activity in the glucuronyl C5-epimerase knock out MEF cells

Tahira Batool[a], Jianping Fang[a,c], Viktor Jansson[a], Hongxing Zhao[b], Caroline Gallant[b], Aristidis Moustakas[a,b], Jin-Ping Li[a,b,*]

[a] Department of Medical Biochemistry and Microbiology, The Biomedical Center, University of Uppsala, Uppsala, Sweden
[b] Science for Life Laboratory Uppsala, The Biomedical Center, University of Uppsala, Uppsala, Sweden
[c] Glyconovo Technologies Co., Ltd., TianXiong Road, Shanghai International Medical Zone (SIMZ), Pudong New Area, Shanghai 201318, China

ARTICLE INFO

Keywords:
BMP signaling
Heparan sulfate
MEF cells
Smad
Glucuronyl C5-epimerase
Bone Morphogenetic Protein

ABSTRACT

Glucuronyl C5-epimerase (Hsepi) catalyzes the conversion of glucuronic acid to iduronic acid in the process of heparan sulfate biosynthesis. Targeted interruption of the gene, *Glce,* in mice resulted in neonatal lethality with varied defects in organ development. To understand the underlying molecular mechanisms of the phenotypes, we used mouse embryonic fibroblasts (MEF) as a model to examine selected signaling pathways. Our earlier studies found reduced activities of FGF-2, GDNF, but increased activity of sonic hedgehog in the mutant cells. In this study, we focused on the bone morphogenetic protein (BMP) signaling pathway. Western blotting detected substantially elevated endogenous Smad1/5/8 phosphorylation in the Hsepi mutant (KO) MEF cells, which is reverted by re-expression of the enzyme in the KO cells. The mutant cells displayed an enhanced proliferation and elevated alkaline phosphatase activitywhen cultured in osteogenic medium. Analysis of the genes involved in the BMP signaling pathway revealed upregulation of a number of BMP ligands, but reduced expression of several Smads and BMP antagonist (*Grem1*) in the KO MEF cells. The high level of Smad1/5/8 phosphorylation was also found in primary calvarial cells isolated from the KO mice. The results suggest that Hsepi expression modulates BMP signaling activity, which, at least partially, is associated with defected molecular structure of heparan sulfate expressed in the cells.

1. Introduction

Signaling activities of numerous growth factors and morphogens, e.g. FGF, TGFβ, BMP, HGF, Wnt, Hh, depend on cell surface receptor systems, which consist of a tyrosine or serine/threonine kinase-type receptor along with heparan sulfate proteoglycan (HSPG) as co-receptor [1]. HSPG is ubiquitously expressed in all tissues, having essential functions in animal development [2,3]. The biological activities of HSPG are mainly through interaction of the side polysaccharide chain, heparan sulfate (HS) with ligands, including growth factors and their receptors [4]. The diverse functions of HS are ascribed to their complicated molecular structure that is generated by a controlled biosynthetic mechanism, varying in tissues and cells. The biosynthetic process is initiated by formation of a polysaccharide chain composed of alternating D-glucuronic acid (GlcA) and *N*-acetylglucosamine (GlcNAc) units that are modified through a series of reactions, including *N*-deacetylation/N-sulfation of GlcNAc residues, C5-epimerization of GlcA to L-iduronic acid (IdoA) units and O-sulfation at various positions of the hexuronic acid and glucosamine residues [4]. The action of glucuronyl C5-epimerase (Hsepi) results in generation of IdoA residues that are found in the sequences binding to protein ligands, and are considered to promote ligand apposition through their conformational flexibility [5]. Targeted disruption of the gene, *Glce*, in mice eliminated the enzyme (Hsepi) expression and resulted in production of abnormal HS structure, completely lacking IdoA residues with severely distorted sulfation pattern. The Hsepi deficient mice are neonatally lethal, with multiple development defects; however, some organs developed seemingly normal [6].

To find out the mechanisms underlying the differential developmental defects of Hsepi mutant mice, we isolated embryonic fibroblasts (MEF) for examining activities of selected growth factors that are known to play essential roles in animal development. Our earlier studies revealed that the MEF cells isolated from the Hsepi mutant (KO) mice displayed reduced FGF2-stimulated signaling activity, due to lower affinity of the mutant HS in binding to FGF-2 [7]. Structural analysis of the HS isolated from the Hsepi KO MEF cells showed, apart

* Corresponding author at: Department of Medical Biochemistry and Microbiology, University of Uppsala, Uppsala, Sweden.
E-mail address: jin-ping.li@imbim.uu.se (J.-P. Li).

https://doi.org/10.1016/j.cellsig.2018.11.010
Received 18 July 2018; Received in revised form 14 November 2018; Accepted 14 November 2018
Available online 17 November 2018
0898-6568/

from complete lack of IdoA, major alteration in the HS structure, including increased N- and 6-O-sulfation and reduced total 2-O-sulfation [7]. Our recent studies showed that lack of Hsepi led to higher Indian hedgehog (Ihh) signaling in mutant chondrocytes during bone development, which is due to reduced expression of Ptch1 and lower affinity of Ihh to the mutant HS expressed in Hsepi-KO cells [8].

One distinct defect of the Hsepi mutant embryos is skeletal malformation [6]. As bone morphogenetic protein (BMP)/transforming growth factor-beta (TGF-β) play crucial role in skeletal development, perturbations of this pathway lead to skeletal abnormalities [9]. To get some insight into the mechanisms behind the skeletal development defects of Hsepi mutants, we examined BMP-signaling in the MEF cells that we have used previously [7]. The results show higher endogenous Smad1/5/8 phosphorylation in the mutant cells (KO MEF), which can be reverted when Hsepi is re-introduced into the cell. Analysis of selected genes involved in the BMP-Smad pathway revealed substantially elevated expression of several BMPs and reduced expression of Smad and BMP receptors. Particularly, the gene of the BMP-2 antagonist, *Grem1*, was significantly downregulated. Putting together, the results show a close correlation of Hsepi expression and BMP signaling, which is presumably associated with the defects in HS molecular structure. The results also suggest that the molecular structure of HS can affect the activity of BMP, which should be considered for the therapeutic application of BMP-2 for treatment of Hereditary Multiple Exostoses (HME) [10], where abnormal HS structure is detected.

2. Results

2.1. Elevated endogenous Smad1/5/8 phosphorylation in the Hsepi KO MEF cells

The primary aim of this study was to get some insight for the severe skeletal development defects in the Hsepi KO mice [6]. WT and KO MEF cells were incubated with or without BMP-2 after starvation for 24 h and Smad1/5/8 phosphorylation was detected by western blotting. The result shows a substantially higher level of p-Smad1/5/8 in the KO cells, even without BMP-2 stimulation when cultured in the starvation media (Fig. 1A). Analysis of cell proliferation using the MTS method revealed a higher proliferation rate of the KO cells (Fig. 1B), which most likely is associated with the 'hyper' endogenous Smad1/5/8 phosphorylation activity. The elevated Smad1/5/8 phosphorylation is not a result of increased expression of the protein, as the amount of Smad1 is apparently even less in the KO cells (Fig. 1A). As BMP signaling plays important roles in bone development, it is rational to assume a correlation of the 'hyper' BMP signaling activity with the abnormal formation of the skeletal system in the mice. Thus, we cultured the MEF cells in the osteogenic medium aiming to differentiate them into the osteogenic lineages [11]. Unfortunately, repeated experiments showed that the cells died after 3 days of culture on the osteogenic medium. Nevertheless, significantly higher level of alkaline phosphatase (ALP) activity in the KO cells cultured in both normal and osteogenic media indicates a tendency of enhanced differentiation (Fig. 1C). The poor response of KO cells to the added BMP-2 is most likely due to the high endogenous activity.

The elevated Smad1/5/8 phosphorylation and higher proliferation rate of the KO cells cultured in starvation medium in the absence of BMP-2 suggest a potential autocrine activity of the cells. To test for the presence of putative BMP family ligands secreted in the medium of the MEFs, we examined Smad pathway activity using a reporter cell line (C2C12-BRE-luc) derived from mouse C2C12 pluripotent cells, expressing the luciferase gene under the control of a synthetic promoter, derived from the mouse *Id1* gene, which responds strongly to BMP-Smad1/5/8 signaling [12]. Analysis of the reporter luciferase activity of the C2C12-BRE-luc cells cultured in the conditioned media of KO and WT cells showed a significantly higher level of luciferase activity of the C2C12 cells cultured in conditioned medium from the KO cells compared to the medium from WT MEFs (Fig. 1D).

To verify that the elevated Smad1/5/8 phosphorylation is through the activation of BMP receptors, we cultured the KO cells in the presence of dorsomorphin homolog 1 (DMH1) that is a selective inhibitor for the type 1 BMP receptors [13]. The results show that DMH1, at concentrations higher than 0.1 μM effectively inhibited the Smad1/5/8 phosphorylation (Supplementary Fig. 1), indicating that the loss of Hsepi in the KO MEFs led to enhanced Smad1/5/8 phosphorylation, at least partly, through activation of type 1 BMP receptors.

To demonstrate that the elevated level of Smad1/5/8 phosphorylation in the KO cells is indeed associated with Hsepi expression, the *Glce* gene was re-introduced to the mutant MEF cells. Detection of the Hsepi activity confirmed success in re-expression of the enzyme (Fig. 2A). Western blotting shows reduced level of Smad1/5/8 phosphorylation in the KO cells re-expressed Hsepi in comparison to mock transfected cells and KO cells (Fig. 2B).

2.2. Disturbed expression of genes and proteins involved in BMP signaling in the Hsepi KO MEFs

The higher cellular activity of the Hsepi KO cells cultured in the starvation medium and the effect of conditioned medium in C2C12-BRE-luc cells led to the hypothesis that the KO cells produced stimulating factors that led to Smad1/5/8 phosphorylation and cell growth. Hence, we chose to examine expression of the genes involved in the BMP-Smad signaling pathway using the Microarray PCR kit. The two independent experiments from two cell cultures showed a significantly increased expression of several cytokines, e.g. BMP-4, 6 and 7 in the KO cells (Fig. 3A, C), and a moderately reduced expression of a few downstream signaling molecules, Smad1, 4 and 7 (Fig. 3B, D). In experiment 1, an increased expression of BMP-2 was detected (Supplementary Fig. 1); this value was lost in experiment 2. There was a slight increase of BMP receptor 1a and 1b (Bmpr1a, b), but a slight reduction of BMP receptor 2 (Bmpr2) in the KO cells (Supplementary Fig. 2). Apart from the cytokines and receptors, *Fst* (follistatin) was substantially upregulated and *Grem1* (gremlin 1) was significantly downregulated. Follistatin is an activin-binding protein, also having inhibitory function against BMPs; while gremlin 1 is a BMP antagonist [14]. The data indicates that lack of Hsepi resulted in a disturbed expression pattern of genes involved in the BMP-Smad signaling pathway.

Further, we employed a Proximity Extension Assay (PEA; [15]) for a highly sensitive multi-panel analysis of proteins expressed in the cells. Restricted by the cost of labeling antibodies, we analyzed only a few proteins that play roles in the BMP signaling pathway. The results confirm the reduced levels of Smad4 and Bmpr2 (Fig. 4). As Runx2 (runt-related transcription factor 2) is a key transcription factor associated with osteoblast differentiation and CDH1 (cadherin-1) plays important roles in cell-cell interactions at early embryonic development, we also examined these two proteins in the cells. Both proteins had a significantly lower level in the KO MEF cells. CDH1 has been reported to regulate craniofacial development [16], the reduced the level of CDH1 may also have contributed to the defects of bone development in the Hsepi KO mice, through affecting BMP signaling pathway.

2.3. Altered expression of genes critical for heparan sulfate biosynthesis

Our earlier study found that heparan sulfate (HS) expressed in the KO MEF cells displayed a lower affinity in binding to FGF2, which was ascribed to the structural alteration of HS due to complete lack of iduronic acid residues, reduced 2-O-sulfation and increased N- and 6-O-sulfation [7]. This was assumed to be due to alteration in the expression of the biosynthesis enzymes. To confirm this and correlate to the observations in this study, we examined the expression of the genes coding for the critical modification enzymes by qPCR. The results demonstrate reduced expression of Hs2st and upregulated expression of

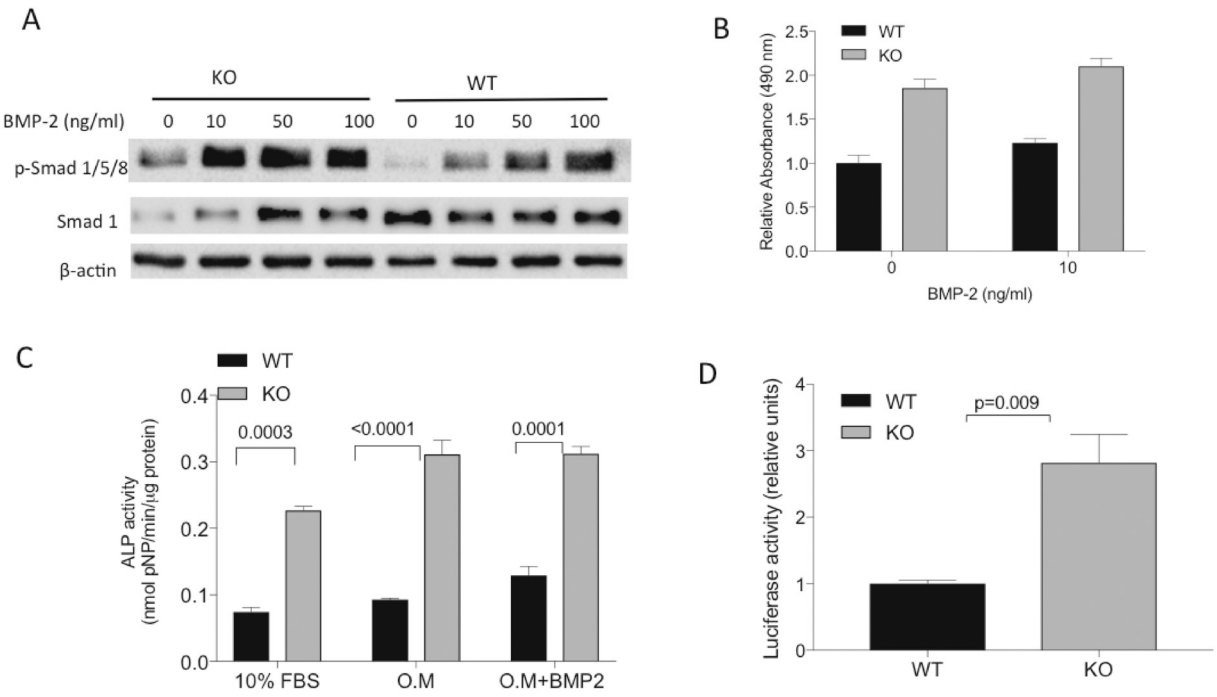

Fig. 1. *Smad phosphorylation and cell proliferation:* (A) MEFs were cultured in starvation medium for 24 h and stimulated with BMP-2 at the indicated concentrations for 30 min. The cell lysates were analyzed by western blotting. (B) Proliferation of MEFs cultured in starvation medium for 24 h with or without addition of BMP-2 was determined by MTS analysis. The proliferation is expressed as relative absorbance normalized to WT without BMP-2 stimulation as 1. (C) Alkaline phosphatase (ALP) activity was determined in the cells cultured in DMEM + 10%FBS and osteogenic medium (O.M.) with or without BMP-2 for 3 days. Average enzymatic activity was normalized to total protein per extract. (D) Luciferase activity of C2C12-BRE-luc cells cultured in the conditioned media from WT and KO cells culture. The luciferase activity was normalized to β-galactosidase activity, set WT as 1. The data plotted in bar graphs represent average values from triplicate determinations with standard deviations. Repeated measures one-way Annova or two-way Annova were applied. Sidak's multiple comparison tests were performed for the data in (C).

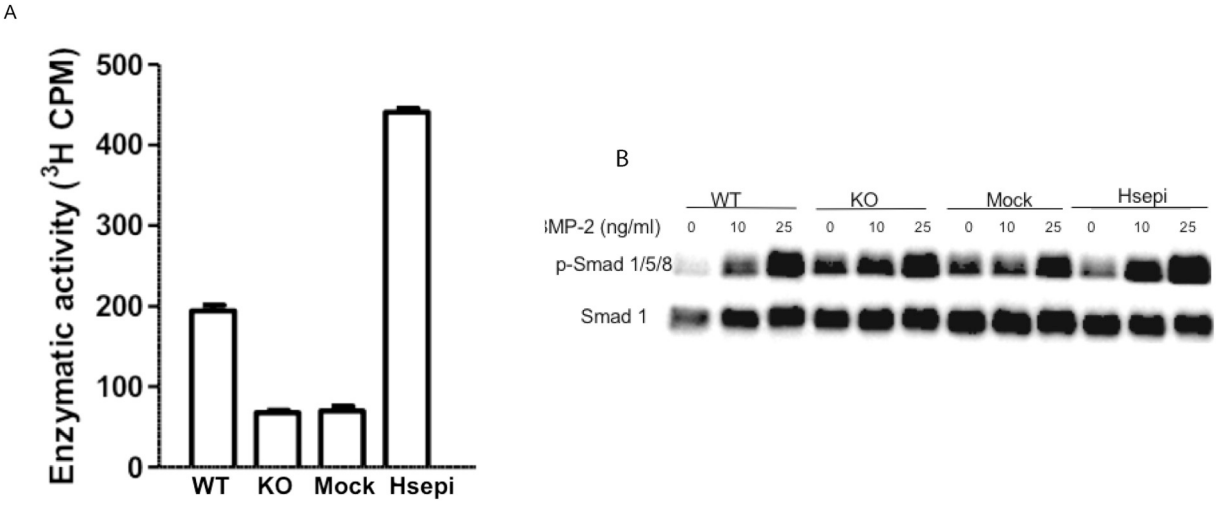

Fig. 2. *Re-expression of Hsepi in the KO MEF cells:* (A) KO MEF cells were stably transfected with the *Glce* gene by a Lenti virus system and Hsepi activity was analyzed. Release of ^{3}H from the substrate was detected in WT and Hsepi (re-expressed), while not in the KO and mock transfected KO (the counts are background); (B) The cells were cultured in starvation medium for 24 h and stimulated with BMP-2 at the indicated concentrations for 30 min. The cell lysates were analyzed by western blotting.

Hs6st1, 3 and Ndst2 (Fig. 5A), which corroborates with our earlier finding of HS structural alteration in the cells [7]. However, in contrast to FGF2, the mutant HS displayed a higher binding capacity to BMP-2 (Fig. 5B), which most likely contributed to the enhanced Smad phosphorylation in the KO cells. Nevertheless, the HS chain length had no difference between the KO and WT-MEFs (Supplementary Fig. 3). Immunocytostaining of the cells showed positive signals of WT cells with a phage display antibody (AO4B08) that recognizes iduronic acid as an epitope (Fig. 5C), which is lacking in the KO cells.

2.4. Higher level of Smad1/5/8 phosphorylation in cultured primary calvarial cells isolated from Hsepi KO embryos

To ascertain that the elevated Smad1/5/8 phosphorylation is not a unique property of the MEF KO cells, we examined BMP-2 signaling activities in primary calvarial cells isolated from embryos of E18.5. Similar to the MEFs, KO calvarial cells displayed a higher Smad1/5/8 phosphorylation in response to BMP-2 stimulation and a lower level of Smad1 (Fig. 6A). Moreover, Western blotting showed lower levels of

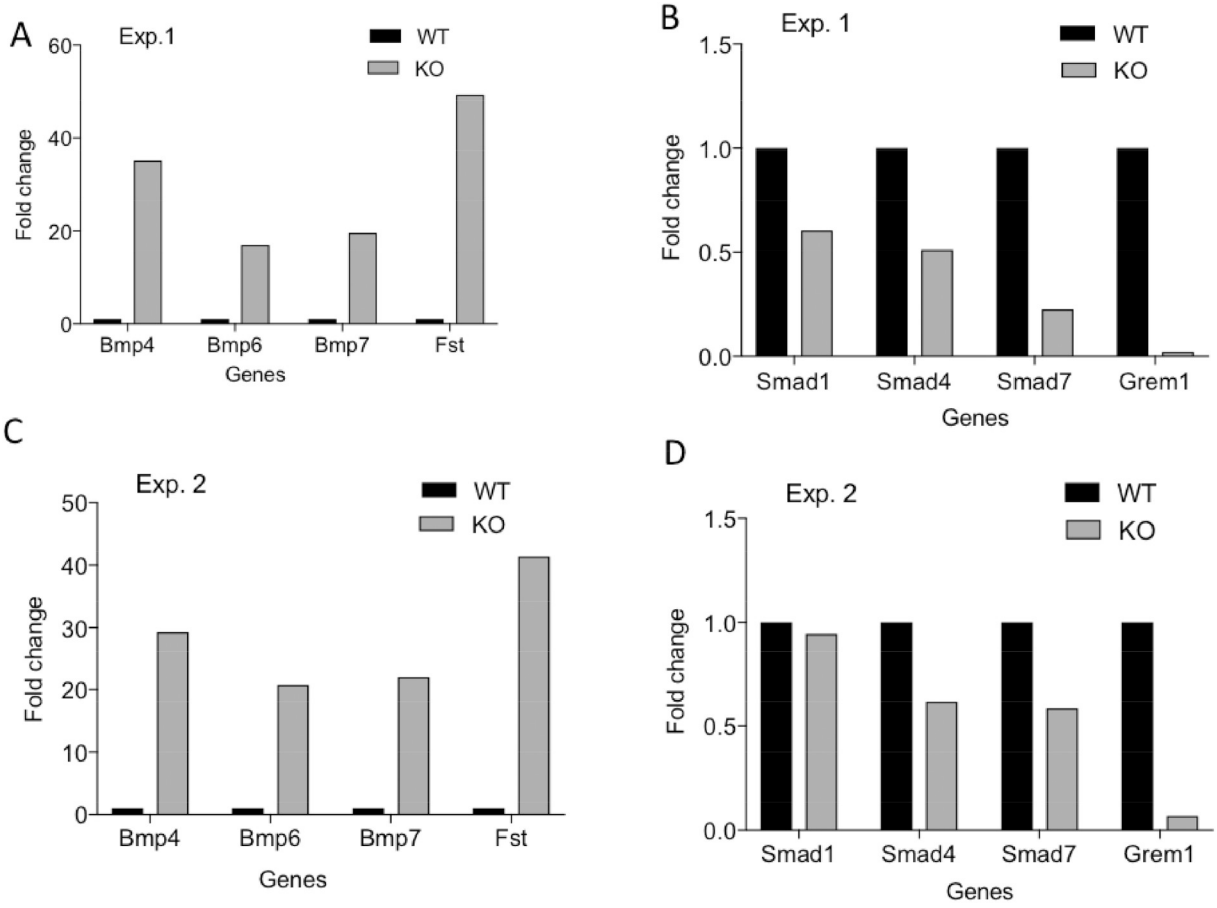

Fig. 3. *Microarray analysis of genes involved in the BMP-Smad signaling pathway:* Both WT and KO cells were cultured for 24 h in DMEM supplemented with 10% FBS and total RNA was isolated for preparation of cDNA. The cDNA (10 ng) was used per reaction of Prime PCR pathway array 96-well plate (Development-BMP signaling M96) using SsoAdvanced universal SYBR Green Supermix. The data from two independent experiments (mean of 6–9 readings per gene) are separately shown. (A, C) shows the genes of elevated expression and (B, D) shows the genes of reduced expression in KO cells. The expression level of WT is set as 1. (For interpretation of the references to colour in this figure legend, the reader is referred to the web version of this article.)

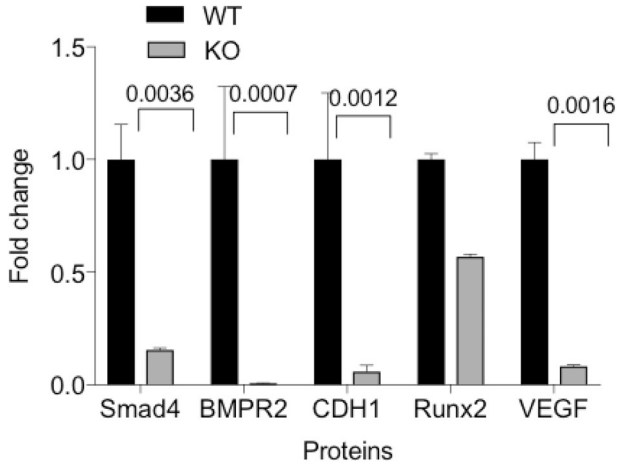

Fig. 4. *PEA analysis of protein expression:* Both WT and KO cells were cultured as above. After lysis in RIPA buffer, 1 µl of the lysate (4000–5000 cells/µl) was used for the PEA analysis with selected antibodies (see method). Protein expression values were determined by subtracting the mean Cq-value (log2 scale) of the lysis buffer control ($n = 3$) plus two standard deviations of the mean minus the Cq-value of the sample. Two-way Annova was applied followed by Sidak's multiple comparison tests.

Runx 2 in the KO calvarial cells cultured in the osteogenic medium (Fig. 6B), which seems resistant to the stimulation of BMP-2. As Runx2 is a key transcription factor associated with osteoblast differentiation, the reduced expression of Runx2 may also have contributed to the defect of skeletal development of the Hsepi mutant animals.

3. Discussion

In this study, we found that glucuronyl C5-epimerase (Hsepi) plays a role in BMP-Smad signaling pathway. It has been stated that about one-third of the approximately 30 members of the TGF-β family bind to heparan sulfate (HS)/heparin [18], employing cell surface HS as a co-receptor by facilitating ligand-induced receptor hetero-oligomerization [19]. One earlier study found that the cells lacking NDST1 (one of the modification enzymes in HS biosynthesis) impaired BMP internalization in lung development [20]. Our study extends the finding and demonstrates that elimination of Hsepi in cells disturbed the BMP signaling pathway through several mechanisms, including upregulation of BMP ligand expression, downregulation of BMP inhibitors and enhanced interaction of HS with BMP ligands. The effect of Hsepi in BMP signaling also has been observed in *Drosophila* [21,22], indicating an evolutionarily conserved role of Hsepi.

The high level of endogenous p-Smad 1/5/8 in the KO cells is believed due to the elevated levels of BMPs that act through activation of the receptors, as application of DMH1 (a type I BMP receptor inhibitor) has attenuated the Smad1/5/8 phosphorylation in the KO cells. A recent study reported that cell-associated HS controls BMP ligand

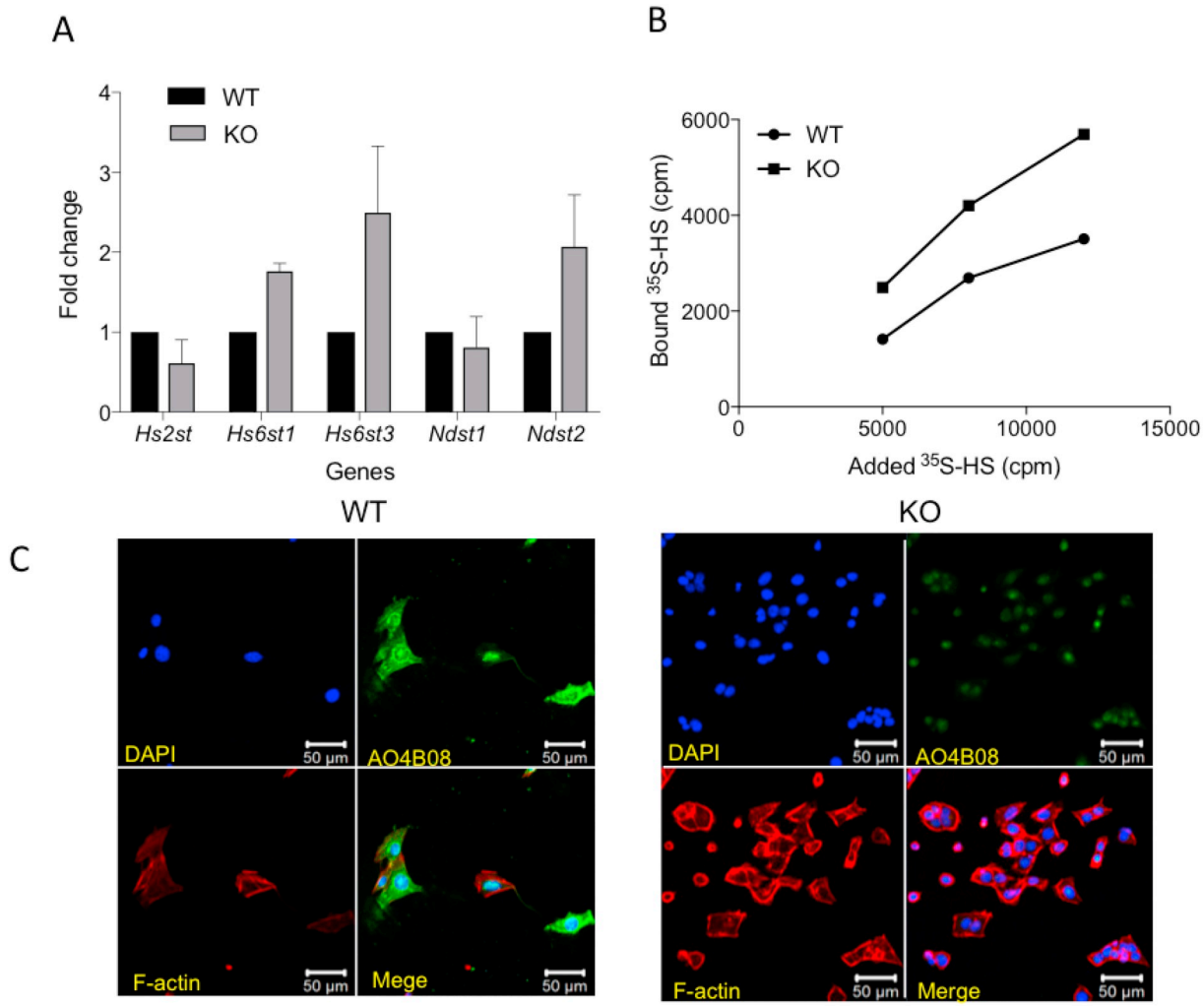

Fig. 5. *Heparan sulfate structure and functions.* (A) Quantification of selected sulfotransferase genes critical for HS biosynthesis by Q-PCR. The c-DNA (10–20 ng) prepared as above was used for the Q-PCR analysis. The primers are listed in Table 1. ΔΔCt versus β-actin was determined. The data represent average ± SEM of 3–6 separate analyses. The expression level of WT was set as 1. (B) Binding of BMP-2 to HS. BMP-2 (1 μg) was incubated with metabolically ^{35}S-labeled HS in the volume of 200 μl at RT for 1 h. Bound HS was trapped on a nitrocellulose filter and recovered for radioisotope counting. The data are average of duplicate analysis. (C) Immunochemical staining of the MEFs with VSV-G tagged phage display antibody (AO4B08; recognizing iduronic acid in HS) [17], followed by incubation with mouse anti-VSV-G antibody, goat anti-mouse IgG coupled with Alexa 488 (green). The F-actin was visualized by staining with Rhodamine Phalloidin (red). The nuclei were stained with DAPI (blue). (For interpretation of the references to colour in this figure legend, the reader is referred to the web version of this article.)

availability and dynamics of its receptor [23], which is dependent on the molecular structure of HS. The higher binding capacity of the mutant HS to BMP-2 probably enhanced the interaction of BMP-2 with its receptors. The increased BMP-stimulated signaling activity most likely has contributed to the intensified calcification in the skull of the Hsepi mutant embryos [6]. This is in the line with the finding that moderate defects or osteochondroma-like outgrowths in the cranial base of Hereditary Multiple Exostoses (HME) patients is associated with enhanced BMP-signaling activity [10].

The most notable finding is the dramatically suppressed expression of *Grem1* in the KO MEF cells. Gremlin 1, a member of the CAN (Cerberus and DAN) family of secreted BMP (bone morphogenetic protein) antagonists, is critical in limb skeleton and kidney development, the two penetrating phenotypes observed in the Hsepi KO mice [6]. Thus, it can be assumed that reduction of gremlin 1 activity may have played important roles for the development defects in the Hsepi KO mice. We will examine the levels of gremlin1 in different organs of the KO embryos, to find out whether gremlin 1 expression is also suppressed in other organs of the mice. Another interesting finding is the upregulated expression of follistatin, which presumably is induced by the high activity of BMP-Smad signaling in the KO cells, causing a negative feedback to inhibit BMP activity. Similarly, the reduced expression of BMP receptors and downstream ligand Smads may also be a negative feedback regulation mechanism, though the molecular interactions remain to be elusive. Furthermore, it is worth to examine a possible biological link between the reduced levels of gremlin 1 and Runx2 as a molecular pathway that links BMP signaling misregulation in the Hsepi KO animals.

It is noteworthy that both gremlin and follistatin bind strongly to HS and heparin [24–26]. It was proposed that gremlin binds to HS on the cell surface and in the ECM, providing for a localized reservoir that modulates BMP activity [27]. Thus, it can be hypothesized that the structural alteration of HS in the KO cells [7] has perturbed its binding capacity to gremlin 1, which sends a negative feedback signal to suppress gremlin 1expression. As gremlin1 plays important roles in cell growth, particularly in cancers, it will be of great interest to find out the correlation of gremlin 1 and HS/Hsepi in cancers, especially, Hsepi has been reported as a tumor suppressor gene in several cancers [28,29].

In conclusion, our results indicate a role of glucuronyl C5-epimerase (Hsepi) in BMP-signaling pathway, and the elevated BMPs activity most likely have contributed to the skeletal development defects of the Hsepi mutant mice [6]. Hypothetically, deletion of Hsepi gene suppressed

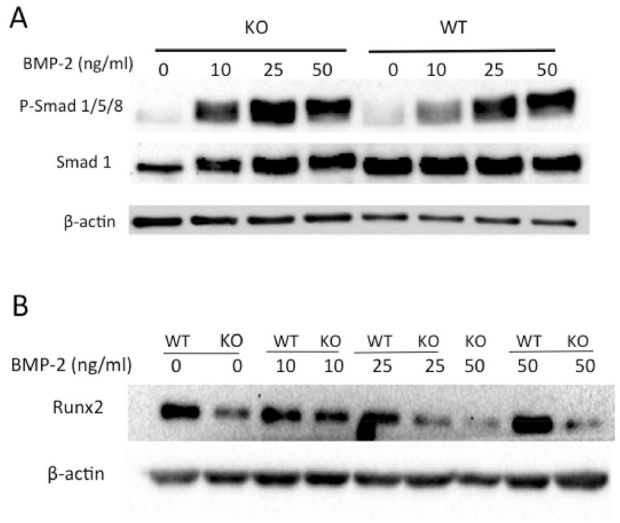

Fig. 6. *Analysis of primary calvarial cells*: (A) The primary cells were isolated from the skull of embryos at E18.5, and cultured in DMEM supplemented with 10% FBS. After starvation for 24 h, the cells were stimulated with BMP-2 at the concentrations indicated for 30 min. The cell lysate was analyzed by western blot for (A) P-Smad1/5/8 and (B) Runx2 with or without stimulation of BMP-2.

gremlin 1 expression, by a yet unknown mechanism, leading to upregulation of BMPs. The high level BMP expression may send feedback signals, stimulating expression of follistatin and down regulation of Smad. The novel finding of Hsepi-gremlin 1 regulation axis should be further explored, since gremlin 1 plays essential roles in stem cell differentiation [30] and is involved in the pathological process of several cancers [31].

4. Materials and methods

The MEF cells were isolated from embryos as reported previously [7]. The wild type cells are referred as WT and the mutant cells referred as KO. The reagents are described in the methods. For re-expression of Hsepi in the KO MEF cells, we have used a same Lentil virus system and method as described [32].

4.1. Isolation and culture of calvarial cells

Embryos on day 18.5 from heterozygote breeding of the Hsepi mice were dissected for isolation of calvarial cells [33]. Briefly, calvaria were dissected from the embryos (2–3 of KO and WT, respectively) and were kept in hanks balanced salt solution followed by digestion with collagenase (Sigma C-9891, crude Type IA) at 37 °C for 15 min with shaking (70–80 rpm). Supernatants were discarded and collagenase digestion was repeated for 30 min. The cells were collected and washed twice with PBS and were treated with EDTA for 15 min at 37 °C with shaking. The cells were then spin down at 400 ×g for 5 min and re-suspended in 1 ml DMEM medium and plated in T-25 flask. For differentiation, the cells were seeded onto 6 well plates at a density of 2–5 × 10^5cells/well in 2 ml of DMEM supplemented with 10%FBS for 48 h. Then the cells were changed to osteogenic medium (Gibco) supplemented with100 μg/ml ascorbic acid phosphate (Sigma) and 10 mM β-glycerol-phosphate (Sigma) with and without addition of BMP-2.

4.2. Cell proliferation

The cells (1000 − 2000) were seeded in 96-well plate and cultured for 24 h, then changed to starvation medium with or without BMP-2 stimulation for 24 h. Cell proliferation was determined by MTS assay (Promega) that measures absorbance at 490 nm using a TECAN Plate reader. The experiments were repeated two times and the results are expressed as the mean ± SE of 2 independent experiments (total of 10 wells).

4.3. Western blotting

Cells were seeded onto 6 well plates at a density of 2–5 × 10^5cells/well in 2 ml of DMEM supplemented with 10% FBS. After 24 h, the medium was replaced by starvation medium (DMEM without FBS) for 24 h. Then the cells were changed to fresh starvation medium with or without addition of BMP-2 at different concentrations. Following stimulation for 30 min, medium was removed and cells were washed twice with PBS before lysis in 100 μl of RIPA buffer (50 mM Tris pH 7.5, 150 mM NaCl, 1%Triton X-100, 1% Nadeoxycholate, 1 mM EDTA and 0.1% SDS, protease inhibitor, 1 mM NaF, 1 mM Na_3VO_4). The lysate was kept on ice 30 min followed by vortex at high speed 5 min and centrifugation at 13,000 rpm for 10 min. The supernatants were collected and protein concentration was determined (BCA assay). Samples (30–50 μg of total protein) were separated by electrophoresis on SDS-PAGE (10%) and electroblotted onto a nitrocellulose membrane. The membrane was probed with antibodies against P-Smad1/5/8 and Smad1 (Cell Signaling Technology), Runx2 as well as β actin. The signals were developed using Super Signal West Duration Substrate (Thermo Scientific) and documented by Bio-Rad CCD camera. Western blot analysis for each protein was repeated more than 2 times of cell culture and one representative blot is shown.

For the inhibitory experiment, starved KO cells were cultured in the presence of dorsomorphin homolog 1 (DMH1) at the concentrations of 0.05–0.5 μM for 24 h. DMH1 was synthesized by the Ludwig Institute for Cancer Research Ltd. Medicinal Chemistry Laboratory, San Diego, USA. The P-Smad1/5/8, total Smad and actin were analyzed as above.

4.4. Luciferase assay

C2C12 cells stably expressing BRE_2-luc and β-gal [34] were cultured in the conditioned medium from WT and KO MEF culture (1:1 ratio mixed with fresh medium) for 48 h. Cells were washed and lysed in 5 mM Tris-phosphate buffer, pH 7.8, containing 2 mM dithiothreitol (DTT), 2 mM CDTA (trans-1,2-diaminocyclohexane-N,N,N′,N′ tetra-acetic acid), 5% glycerol and 1% Triton X-100. Luciferase reporter assay was performed with the enhanced firefly luciferase assay kit (Biotium Inc.), following the protocol of the manufacturer. β-Galactosidase activity was assayed by mixing the cell lysate with 100 mM sodium phosphate pH 7.3, 1 mM $MgCl_2$, 50 mM β-mercaptoethanol and 0.67 mg/ml of ONPG (*O*-Nitrophenyl β-D-Galactopyranoside) and the absorbance was measured at 420 nm. The cellular activity of C2C12-BRE-luc was expressed as the promoter activity (BRE-luciferase) that is normalized by the ratio of luciferase and β-galactosidase activity.

4.5. Alkaline phosphatase (ALP) assay

Cells were plated in 6-well plate at a density of 2 × 10^5 cells/well in DMEM, 10% FBS. At the confluency of 70–80%, cells were transferred into osteogenic medium (Gibco) supplemented with100 μg/ml ascorbic acid phosphate (Sigma) and 10 mM β-glycerol-phosphate (Sigma) with and without 300 ng/ml BMP-2. Alkaline Phosphatase Diethanolamine Activity kit (AP0100) was used to measure ALP activity following the instruction. Briefly, the cells were washed with PBS and lysed in an ALP lysis buffer (1 mM $MgCl_2$, 0.1 mM $ZnCl_2$, 100 mM glycine, pH 10.5). The lysate was kept on ice for 30 min followed by vortex at high speed for 5 min and centrifugation at 13,000 rpm for 10 min. The lysate of 20 μl (40–60 μg of total protein) of supernatant was transferred into a 96-well plate, each sample in three wells. The substrate solution was prepared by mixing the reaction buffer (1.0 M Diethanolamine, 0.5 mM $MgCl_2$, pH 9.8) with freshly prepared 0.67 M *p*-Nitrophenyl Phosphate (pNPP) solution and kept on ice. After adding 100 μl of the substrate

solution to the samples, absorbance was immediately measured at 405 nm at room temperature and reaction progress was monitored for 20 min with 5 min intervals. Units/ml were calculated according to formula below.

4.6. Microarray analysis of gene expression

Cells were seeded in 6-well plate at density 3×10^5cells/well. After 24 h, the cells were collected for RNA isolation and c-DNA synthesis following the protocol of iScript cDNA synthesis kit and iScript cDNA reverse transcription supermix for RT-qPCR (BioRad), respectively. RNA (2 μg) was converted to c-DNA in 100 μl, of which 10 ng/μl was used per reaction of Prime PCR pathway array 96-well plate (Development-BMP signaling M96, #10030738) using SsoAdvanced universal SYBR Green supermix. The data was from two independent experiments.

4.7. Quantification of gene expression by qPCR

The cDNA prepared above were used for analysis of genes encoding for enzymes committed to HS biosynthesis (Ndst1, Ndst2, *N*-deacetylase/N-sulfotransferases; Hs2st, HexA 2-O-sulfotransferase; Hs6st1–3, GlcN 6-O-sulfotransferases) by qPCR. Values of WT-MEF cells are given as one and the values of KO cells are expressed as fold-change. The primers used for the q-PCR are listed in Table 1.

4.8. Proximity extension assay (PEA) analysis

For generation of PEA probes, antibody-oligonucleotide conjugation was performed using click conjugation chemistry. Briefly, 30 μg (2 μg/μl in PBS) of polyclonal antibodies (R&D systems) were activated with 2 mM dibenzylcyclooctne-NHS ester (DBCO; Sigma-Aldrich) in a mole ratio of 1:16.5 for 30 min at RT. The reaction was stopped by adding 1 M Tris to a final concentration of 100 mM. Unreacted DBCO was removed by a 7-kDa Zeba column (Thermo Fisher Scientific). Antibodies were then split into two parts, and a unique A oligonucleotide or a common universal B oligonucleotide was added in a mole ratio of 1:1.75 (antibody:oligo). These oligonucleotides (Integrated DNA Technologies, Leuven, Belgium) were synthesized with a 5′-azide modification, and contain one site for pair-wise annealing between the A and B oligonucleotide, one universal site for binding of molecular beacon and two primer sites for PCR amplification and qPCR detection. The details of the oligonucleotides are published [35]. Unconjugated oligos were depleted by DBCO magnetic beads (Jena Bioscience, Germany) overnight at 4 °C. To the B universal oligonucleotide, an 89-mer oligonucleotide was hybridized and added at molar ratio of 2:1. Seven A or B oligocleotide-antibody probes were pooled separately and diluted to 1.33 nM in Probe Diluent plus 0.02% NaN_3. For proximity extension and detection, one μl of cell lysate (4000 or 5000 cells/μl) was mixed with 0.3 μl of 7-plex proximity A and B probe mix, 0.3 μL PBS and 2.1 μl Incubation Solution and incubated overnight at 4 °C. Extension solution (96 μl) containing 10 μl PEA Solution, 0.5 μl PEA Enzyme, 0.2 μl PCR Polymerase and 85.3 μl water was added to each reaction at RT. After mixing and a maximum 5 min incubation, the tubes was transferred to a thermocycler (Applied Biosystem 2720) running an initial oligonuleotide extension step (50 °C, 20 min), immediately followed by a hot-start step (95 °C, 5 min) and 17 cycles of pre-amplification (95 °C, 30 s; 54 °C, 1 min; 60 °C, 1 min). The extension solution contains universal flanking primers that amplify all 9 sequences in parallel. Finally, 2.5 μL of the preamplification products were mixed with 7.5 μL buffer containing 1 μL 10× PCR Solution (Thermo Fisher), 2.5 mM $MgCl_2$, 0.2 mM dNTP, 1.6 μM ROX, 0.25 μM molecular beacon (FAM –CCCGCTCGCTTATGCTACCGTGACCTGCGAA TCCCGAGCGGG - DABSYL), 0.5 units Uracil-DNA glycosylase (DNA Gdansk), and 0.03 units Platinium Taq Polymerase (Thermo Fisher). The quantitative PCR was run as follows: 25 °C, 30 min, Hot-start (95 °C, 5 min), PCR Cycle 40 cycles (95 °C, 15 s; 60 °C, 1 min). Protein expression values were determined by subtracting the mean Cq-value (log2 scale) of the lysis buffer control ($n = 3$) plus two standard deviations of the mean minus the Cq-value of the sample [= (mean $Cq_{background}$ + 2 mean Cq $SD_{Background}$)-mean Cq_{sample}].

Table 1
The primers used for Q-PCR.

Gene	Forward primer	Reverse primer
Hs2st	*TATGATGCCGCCCAAGTTG*	*CTGTTCAATTTCTCGGACTTCGT*
Hs6st1	*CGGACCCACATTACGAGAAAA*	*GATTGGGCCGATAGCAGGTG*
Hs6st3	*GATGAAAGGTTCAACAAGTGGC*	*CGAAGTTGGTGCATGAGCTG*
Ndst1	*CCACAACTATCACAAAGGCATCG*	*GAAAGGTGTACTTTAGGGCCAC*
Ndst2	*CTGCTGATTGGTTTCAGTCTTGT*	*CCACTGCTACTACAGTCTCCC*

4.9. Metabolic labeling of HS and binding assay

The KO and WT MEF cells were cultured to 95% confluence and $Na^{35}SO_4$ (specific activity 1500 Ci·mmol^{-1}, Perkin Elmer, Waltham, MA, USA) was added to the culture (100 μCi/ml) for 24 h before harvesting. Proteoglycans was purified from cell fractions essentially as described [7]. Briefly, the cells were lysed in buffer containing 1% Triton X-100, 50 mM Tris-HCI, pH 7.4, 0.25 M NaCl, and centrifuged. The cell lysates were applied to a DEAE-Sephacel column (GE Healthcare Biosciences) pre-equilibrated with 50 mM Tris-HCl, 0.25 M NaCl, pH 7.4. The column was washed with 50 mM NaAc, 0.25 M NaCl, pH 4.5 and the bound materials were eluted with 50 mM NaAc containing 2 M NaCl, pH 4.5. The eluted material was desalted on a PD-10 column (GE Healthcare Biosciences), followed by lyophilization to a small volume (400 μl). The samples were treated with Chondroitinase ABC (0.1 U per sample, Seikagaku) to degrade chondroitin sulfate (CS). The HS chains were released from HSPG by alkali treatment in 0.5 M NaOH on ice. The samples were applied again on a 0.5 ml DEAE-Sephacel column to remove CS disaccharide. The HS was desalted in a PD-10 column and lyophilized to 100 μl. The products were analyzed by size exclusion chromatography on a Superose 12 column eluted in the buffer of Tris-HCl, pH 7.4 containing 0.5 M NaCl and 0.1% Triton X-100. The fractions of 0.5 ml were collected and counted after adding 2 ml of scintillation cocktail.

The binding of BMP-2 with HS was determined using a filtration assay method [7], by incubation of BMP-2 (1 μg) in 200 μl of PBS containing 0.2% BSA with ^{35}S-labeled HS at 37 °C for 1 h. The experiment was performed in duplicates.

4.10. Immunocytochemistry

The cells grown on poly-L-lysine-coated coverslips were rinsed with PBS, fixed for 15 with 4% PFA in PBS, and blocked with 0.3% Triton X-100 in PBS containing 3% BSA. The cells were then incubated with a VSV-G tagged phage display antibody (AO4B08; recognizing iduronic acid in HS), followed by incubation with mouse anti-VSV-G antibody, goat anti-mouse IgG coupled with Alexa 488 (Invitrogen). The F-actin probe was visualized by staining with Rhodamine Phalloidin (Cytoskeleton, Inc.). Finally, the coverslips were mounted with Vectashield mounting medium containing 4, 6-diamidino-2-phenylindole (DAPI) for nuclear staining (Vector Laboratories). The digital images were captured with a Zeiss LSM 700 confocal scanning microscope.

4.11. Determination of Hsepi activity

Hsepi activity was analyzed based on the release of ^{3}H (as ^3H_2O) from a C5-^{3}H-labeled polysaccharide substrate, essentially as described [36]. Cells at 90% confluence were lysed in homogenization buffer (50 mM HEPES pH 7.4, 100 mM KCl, 1% Triton X-100, 15 mM EDTA,

containing protease inhibitors) and incubated on ice for 30 min. After centrifugation, total protein in the lysates was determined by the BCA assay (Thermo Scientific), and then mixed with the substrate (5000 cpm). Following incubation at 37 °C for 60 min, released $^{3}H_2O$ was quantified by scintillation counting.

Conflict of interest

Authors declare there is no conflict of interest.

Author contribution

Batool T, Fang J and Li JP designed the study, analyzed the data; Batool T and Fang J performed the experiments; H. Zhao and C. Gallant performed PEA analysis; Batool T, Moustakas A and Li JP wrote the MS.

Acknowledgments

This work was supported by grants from Swedish Cancer Foundation (CAN2015/496), Swedish Research Council (2015-02595), SciLifeLab platform and the Erasmus Mundus Experts4Asia Program (scholarship to Tahira Batool). The authors thank Andrew Shiau, Ludwig Institute for Cancer Research Ltd Medicinal Chemistry Laboratory, San Diego, USA, for DMH1 synthesis and Peter ten Dijke, Leiden University Medical Center, The Netherlands, for C2C12-BRE-luc reporter cells. The Q-PCR primers were kindly shared by Dr. Gunilla Westermark (MCB, UU).

Appendix A. Supplementary data

Supplementary data to this article can be found online at https://doi.org/10.1016/j.cellsig.2018.11.010.

References

[1] X. Lin, Functions of heparan sulfate proteoglycans in cell signaling during development, Development 131 (24) (2004) 6009–6021.
[2] H. Nakato, J.P. Li, Functions of Heparan Sulfate Proteoglycans in Development: Insights from Drosophila Models, Int. Rev. Cell Mol. Biol. 325 (2016) 275–293.
[3] F.E. Poulain, H.J. Yost, Heparan sulfate proteoglycans: a sugar code for vertebrate development? Development 142 (20) (2015) 3456–3467.
[4] J.P. Li, M. Kusche-Gullberg, Heparan sulfate: biosynthesis, structure, *and Function*, Int. Rev. Cell Mol. Biol. 325 (2016) 215–273.
[5] B. Casu, U. Lindahl, Structure and biological interactions of heparin and heparan sulfate, Adv. Carbohydr. Chem. Biochem. 57 (2001) 159–206.
[6] J.P. Li, et al., Targeted disruption of a murine glucuronyl C5-epimerase gene results in heparan sulfate lacking L-iduronic acid and in neonatal lethality, J. Biol. Chem. 278 (31) (2003) 28363–28366.
[7] J. Jia, et al., Lack of L-iduronic acid in heparan sulfate affects interaction with growth factors and cell signaling, J. Biol. Chem. 284 (23) (2009) 15942–15950.
[8] T. Dierker, et al., Altered heparan sulfate structure in Glce(−/−) mice leads to increased Hedgehog signaling in endochondral bones, Matrix Biol. 49 (2016) 82–92.
[9] V.S. Salazar, L.W. Gamer, V. Rosen, BMP signalling in skeletal development, disease and repair, Nat. Rev. Endocrinol. 12 (4) (2016) 203–221.
[10] S. Sinha, et al., Unsuspected osteochondroma-like outgrowths in the cranial base of Hereditary Multiple Exostoses patients and modeling and treatment with a BMP antagonist in mice, PLoS Genet. 13 (4) (2017) e1006742.
[11] K. Dastagir, et al., Murine embryonic fibroblast cell lines differentiate into three mesenchymal lineages to different extents: new models to investigate differentiation processes, Cell Reprogram 16 (4) (2014) 241–252.
[12] O. Korchynskyi, P. ten Dijke, Identification and functional characterization of distinct critically important bone morphogenetic protein-specific response elements in the Id1 promoter, J. Biol. Chem. 277 (7) (2002) 4883–4891.
[13] A. Ao, et al., DMH1, a novel BMP small molecule inhibitor, increases cardiomyocyte progenitors and promotes cardiac differentiation in mouse embryonic stem cells, PLoS One 7 (7) (2012) e41627.
[14] L. Zakin, E.M. De Robertis, Extracellular regulation of BMP signaling, Curr. Biol. 20 (3) (2010) R89–R92.
[15] E. Assarsson, et al., Homogenous 96-plex PEA immunoassay exhibiting high sensitivity, specificity, and excellent scalability, PLoS One 9 (4) (2014) e95192.
[16] R. Shao, et al., Cdh1 regulates craniofacial development via APC-dependent ubiquitination and activation of Goosecoid, Cell Res. 26 (6) (2016) 699–712.
[17] S. Kurup, et al., Characterization of anti-heparan sulfate phage display antibodies AO4B08 and HS4E4, J. Biol. Chem. 282 (29) (2007) 21032–21042.
[18] C.C. Rider, B. Mulloy, Heparin, Heparan Sulphate and the TGF-beta Cytokine Superfamily, Molecules 22 (5) (2017).
[19] W.J. Kuo, M.A. Digman, A.D. Lander, Heparan sulfate acts as a bone morphogenetic protein coreceptor by facilitating ligand-induced receptor hetero-oligomerization, Mol. Biol. Cell 21 (22) (2010) 4028–4041.
[20] Z. Hu, et al., NDST1-dependent heparan sulfate regulates BMP signaling and internalization in lung development, J. Cell Sci. (122) (2009) 1145–1154 Pt 8.
[21] O. Shimmi, et al., The crossveinless gene encodes a new member of the Twisted gastrulation family of BMP-binding proteins which, with short gastrulation, promotes BMP signaling in the crossveins of the Drosophila wing, Dev. Biol. 282 (1) (2005) 70–83.
[22] K. Dejima, et al., Analysis of Drosophila glucuronyl C5-epimerase: implications for developmental roles of heparan sulfate sulfation compensation and 2-O-sulfated glucuronic acid, J. Biol. Chem. 288 (48) (2013) 34384–34393.
[23] C. Mundy, et al., Heparan sulfate antagonism alters bone morphogenetic protein signaling and receptor dynamics, suggesting a mechanism in hereditary multiple exostoses, J. Biol. Chem. 293 (20) (2018) 7703–7716.
[24] A.J. Tatsinkam, B. Mulloy, C.C. Rider, Mapping the heparin-binding site of the BMP antagonist gremlin by site-directed mutagenesis based on predictive modelling, Biochem. J. 470 (1) (2015) 53–64.
[25] C.A. Innis, M. Hyvonen, Crystal structures of the heparan sulfate-binding domain of follistatin. Insights into ligand binding, J Biol Chem 278 (41) (2003) 39969–39977.
[26] F. Zhang, et al., Analysis of the interaction between heparin and follistatin and heparin and follistatin-ligand complexes using surface plasmon resonance, Biochemistry 51 (34) (2012) 6797–6803.
[27] A.J. Tatsinkam, et al., The binding of the bone morphogenetic protein antagonist gremlin to kidney heparan sulfate: such binding is not essential for BMP antagonism, Int. J. Biochem. Cell Biol. 83 (2017) 39–46.
[28] E.E. Rosenberg, et al., D-glucuronyl C5-epimerase cell type specifically affects angiogenesis pathway in different prostate cancer cells, Tumour Biol. 35 (4) (2014) 3237–3245.
[29] E.V. Grigorieva, et al., D-glucuronyl C5-epimerase suppresses small-cell lung cancer cell proliferation in vitro and tumour growth in vivo, Br. J. Cancer 105 (1) (2011) 74–82.
[30] D.L. Worthley, et al., Gremlin 1 identifies a skeletal stem cell with bone, cartilage, and reticular stromal potential, Cell 160 (1–2) (2015) 269–284.
[31] G.S. Karagiannis, et al., Bone morphogenetic protein antagonist gremlin-1 regulates colon cancer progression, Biol. Chem. 396 (2) (2015) 163–183.
[32] J. Fang, et al., Enzyme overexpression - an exercise toward understanding regulation of heparan sulfate biosynthesis, Sci. Rep. 6 (2016) 31242.
[33] Bakker, A. and J. Klein-Nulend, Osteoblast Isolation from Murine Calvaria and Long Bones. vol. 816: p. 19–29.
[34] E. Raja, et al., The protein kinase LKB1 negatively regulates bone morphogenetic protein receptor signaling, Oncotarget 7 (2) (2016) 1120–1143.
[35] M. Lundberg, et al., Homogeneous antibody-based proximity extension assays provide sensitive and specific detection of low-abundant proteins in human blood, Nucleic Acids Res. 39 (15) (2011) e102.
[36] A. Hagner-McWhirter, et al., Biosynthesis of heparin/heparan sulfate: kinetic studies of the glucuronyl C5-epimerase with N-sulfated derivatives of the Escherichia coli K5 capsular polysaccharide as substrates, Glycobiology 10 (2) (2000) 159–171.